Combustion and Flame 193 (2018) 481–490

Contents lists available at ScienceDirect

Combustion and Flame

journal homepage: www.elsevier.com/locate/combustflame

Characterization of thermodiffusive and hydrodynamic mechanisms on the cellular instability of syngas fuel blended with CH_4 or CO_2

Denis Lapalme[a,b,*], Fabien Halter[b,1], Christine Mounaïm-Rousselle[b], Patrice Seers[a]

[a] Laboratoire TFT, École de technologie supérieure, 1100 Notre-Dame Ouest, Montréal, QC H3C 1K3, Canada
[b] Université d'Orléans, Laboratoire PRISME, Orléans, France

ARTICLE INFO

Article history:
Received 1 November 2017
Revised 25 December 2017
Accepted 23 March 2018

Keywords:
Cellularity
Hydrodynamic instability
Thermodiffusive effects
Syngas

ABSTRACT

Thermodiffusive and hydrodynamic instabilities cause a departure from laminar combustion and, as such, are responsible for flame self-acceleration behavior. Due to the presence of hydrogen, syngas is a fuel prone to instabilities and is frequently diluted with CO_2 or co-fired with CH_4. This paper, thus presents an experimental study on how syngas mixed with CO_2 and/or CH_4 influence the onset of both kinds of instability. First, the results show that the laminar flame thickness is the controlling parameter in determining the critical radius at which cellularity appeared when CH_4 is added to syngas. Moreover, higher levels of CO_2 dilution translated into a constant critical radius, illustrating that the thermodiffusive mechanism is counterbalanced by the hydrodynamic one. To help differentiate between both kinds of instability, it is suggested herein to use the coefficient of self-acceleration or the ratio of the flame speed at the critical flame radius on the laminar flame speed. Finally, a correlation predicting the onset of cellularity is proposed based on the equation format proposed by Jomaas et al. (2007), derived from the stability analysis of a spherically expending flame. The correlation expresses the critical Peclet as a function of hydrodynamic and thermodiffusive instabilities and was successfully validated against experimental data from this study and the literature.

1. Introduction

Hydrogen-based fuels, such as syngas (or synthetic gas), are being recognized as attractive alternatives with low environmental impact. Syngas can be produced by the gasification of coal or biomass and used in integrated gasification combined cycle (IGCC) for power generation. Its uses in internal-combustion engines have also been explored [1–3]. Syngas constituents vary greatly as a function of the feedstock and the gasification process [4]. The main components are hydrogen (H_2) and carbon monoxide (CO), but carbon dioxide (CO_2), nitrogen (N_2) [5] and methane (CH_4) [6] are frequent by-products. In some instance, syngas can also be co-fired with methane (CH_4) [5]. As H_2, a major constituent of syngas, is known to develop cellular instabilities, understanding how and when such instabilities could develop is important, since they are responsible for wrinkling flame fronts and creating self-accelerating flame [7]. It also induces turbulence in the unburned mixtures and leads to engine knock [8]. First, a review about the cellularity phenomenon is done for different types of gaseous fuels.

There are three mechanisms generating cellular instabilities, namely hydrodynamic instability, diffusional-thermal instability, and buoyancy-driven instability [9]. The impact of the latter is not significant and can be neglected due to the high flame speed of H_2-based fuels [10]. Hydrodynamic instability is caused by the density jump across the flame while diffusional-thermal instability is caused by the competition between the thermal diffusivity and the mass diffusivity. The ratio between the thermal and mass diffusivities is called the Lewis number $\left(Le = \lambda/\rho C_p D\right)$.

The onset of cellularity has been studied experimentally mostly with lean H_2 and rich propane (C_3H_8) [7,11–13], two non-equidiffusive fuels ($Le \neq 1$). Diffusional-thermal instability of the lighter-than-air hydrogen increased rather linearly by *decreasing* the equivalence ratio φ ($Le < 1$ for lean mixtures), while it increased by *increasing* φ in the heavier-than-air propane ($Le < 1$ for rich mixtures). Meanwhile, hydrodynamic instabilities of H_2 and C_3H_8 peaked at $\varphi \sim 1.1$ due to variations in flame thickness and the thermal-expansion ratio. There is therefore a competition between the two types of instabilities seemingly dominated by diffusional-thermal instabilities [11], since the critical radius of H_2 (C_3H_8) decreased with decreasing (increasing) φ. Earlier onset of

---

[*] Corresponding author at: TFT Laboratory, École de technologie supérieure, 1100 Notre-Dame Ouest, Montréal, QC H3C 1K3, Canada.
E-mail address: denis.lapalme.1@ens.etsmtl.ca (D. Lapalme).

[1] Present address: CNRS–ICARE, Orléans, France.

https://doi.org/10.1016/j.combustflame.2018.03.028

cellularity was observed when H_2 was added to lean and slightly rich C_3H_8 [14,15] or methane [16] flames. This faster appearance of cellularity was associated with a decrease in Lewis number and flame thickness (δ_L). The impact of adding small concentrations of C_3H_8 to H_2 was studied by [14], who observed that the flame became progressively more stable as φ increased for a constant concentration of C_3H_8, illustrating the dominating effect of H_2 on cellularity.

The effects of hydrocarbon addition (CH_4, C_3H_8 and C_4H_{10}) [17], diluent addition (CO_2, N_2 and He) [18], and the variation of the H_2/CO [8,10] on the hydrodynamic and thermodiffusive instabilities leading to cellularity in syngas were studied in a series of papers by Vu et al. Their main conclusion was that H_2 enrichment promotes instabilities by enhancing both the hydrodynamic and diffusional-thermal effects, while adding CH_4, CO, CO_2, or N_2 do not significantly impact the cellularity behavior of the mixtures due to a relatively constant *Le*.

The onset of cellularity represents a departure from laminar combustion as the growth of cells greatly increases the flame surface and is thus associated with a rise in the flame propagation speed though a self-acceleration process [7,19–22]. Yet, results so far show that this self-acceleration is smaller [23–26] than the acceleration induced by turbulence [25,27]. Meanwhile, the specific impact of the hydrodynamic and thermodiffusive mechanisms on self-acceleration has been investigated only recently by [26].

This paper aims at providing more experimental data to enhance the understanding of the phenomena associated with self-accelerating cellular flames. More specifically, it aims at (1) describing the impact of CH_4 or CO_2 addition on the critical radius of a syngas flame; (2) distinguishing between thermodiffusive and hydrodynamic instabilities based on basic flame properties using the phenomena of self-acceleration, and (3) investigating the possibility of correlating the onset of cellularity.

R=10.1 mm	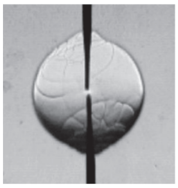
R=11.2 mm	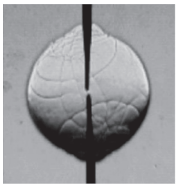
R=12.4 mm	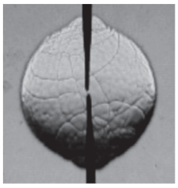
R=13.6 mm	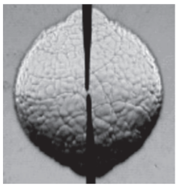
	Le_{eff} = 0.96 σ = 6.89 δ_L (mm) = 0.0268

Fig. 1. Sequence of consecutive images showing the apparition of the hydrodynamic instabilities on a H_2/CO flame.

2. Experimental setup

The experiments were conducted in a cylindrical constant-volume chamber having an internal diameter of 300 mm and a length of 330 mm. Optical accesses to the chamber were provided by two opposite and transparent 40-mm-radius sapphire windows located in the flat sides of the vessel. Once a vacuum was created in the chamber, it was filled with the different gases (purity levels: H_2 – 99.999%, CO – 99.5%, CO_2 – 99.9%, CH_4 – 99.9%, air – hydrocarbon free) until the volume of each gas required to create the desired premix mixture was reached. The volumetric flows of the gases were measured by separate mass-flow controllers (OMEGA FMA 5400, accuracy of ± 1.5% full scale, repeatability of ± 0.5% full scale) and then thoroughly mixed in the gas line before being sent to the chamber. The flow rates were adjusted to ensure the required volume of each gas was reached in the same time lap. All experiments were performed at an initial temperature of 298 K and at 3 atm. Each mixture was tested thrice; the average is provided herein.

The mixture was spark-ignited at the center of the vessel by two tungsten electrodes, creating an outwardly propagating flame (OPF), which quenched when touching the chamber walls. The flame propagation was imaged using a Z-type Schlieren photography setup comprising a pair of 108-mm-diameter mirrors and recorded by a high-speed C-MOS camera (Phantom V9.1) operating at 9800 images per second with a resolution of 352 × 352 pixel^2. Flame development was relatively spherical, although bulges were visible where the flame was in contact with the electrodes, as it can be seen in Fig. 1. Hence, once the bulges are removed, the flame front can be represented by the equation of a circle with a radius *R*. A flame-edge-detection methodology was developed to retrieve *R*. It consists of 4 steps: (1) a background subtraction to reduce the noise, (2) similar to Kelley et al. [28], a withdrawal of a 20° triangular area of the flame on each side of the two electrodes to eliminate the bulges, (3) an edge-detection of the flame disk localized based on the maximum intensity of the post-subtraction image, and (4) identification of the smallest circle bounding the flame disk, yielding *R*. All acquired images were post-processed to obtain the evolution of the flame radius as a function of the time (t) to extract, through Eq. (1), the burning speed S_b, from the burned boundary. Note that the calculations were limited to flames with radii between 6 and 35 mm to avoid the disturbances caused by ignition and wall interference.

$$S_b = \frac{dR}{dt} \tag{1}$$

Finally, from the determination of *R* as a function of time, it was possible to identify the critical flame radius (R_{cr}) which will be described and discussed in the next section. R_{cr} is subjected to uncertainty from the scaling factor, allowing for the conversion from pixel to mm in the flame-edge detection code, and from the choice of the frame at which R_{cr} is reached. The scaling was repeated 6 times and yielded a repeatability error of 1%. Following [12], the uncertainty on the frame at which R_{cr} was observed is considered to be of ± 1 frame, meaning that R_{cr} could be within a frame of the chosen one as instability could appear between images. A faster flame has a greater uncertainty since there is a greater difference of radius between two frames. These two sources of error have been summed following square root method. In the end, the